Minimal nanodisc without exogenous lipids for stabilizing membrane proteins in detergent-free buffer

Dimitri Salvador, Marie Glavier, Guy Schoehn, Gilles Phan, Jean-Christophe Taveau, Marion Decossas, Sophie Lecomte, Sébastien Mongrand, Cyril Garnier, Isabelle Broutin, et al.

BBA - Biomembranes 1861 (2019) 852–860

Contents lists available at ScienceDirect

BBA - Biomembranes

journal homepage: www.elsevier.com/locate/bbamem

Minimal nanodisc without exogenous lipids for stabilizing membrane proteins in detergent-free buffer

Dimitri Salvador[a,b,1], Marie Glavier[a,b,1], Guy Schoehn[c], Gilles Phan[d], Jean-Christophe Taveau[a,b], Marion Decossas[a,b], Sophie Lecomte[a,b], Sébastien Mongrand[e], Cyril Garnier[d], Isabelle Broutin[d], Laetitia Daury[a,b,2], Olivier Lambert[a,b,*,2]

[a] Univ. Bordeaux, CBMN UMR 5248, Bordeaux INP, F-33600 Pessac, France
[b] CNRS, CBMN UMR5248, F-33600 Pessac, France
[c] Université Grenoble Alpes, CNRS, CEA, Institute for Structural Biology (IBS), 38000, Grenoble, France
[d] Laboratoire de Cristallographie et RMN Biologiques, UMR 8015, CNRS, Université Paris Descartes, Faculté de Pharmacie, 4 Avenue de l'Observatoire, 75006 Paris, France
[e] Laboratoire de Biogènese Membranaire, UMR 5200, CNRS, Université de Bordeaux, 71 Avenue Edouard Bourlaux, 33883 Villenave d'Ornon Cedex, France

ARTICLE INFO

Keywords:
Membrane protein
Nanodisc
Lipids
CryoEM

ABSTRACT

Membrane protein stabilization after detergent solubilization presents drawbacks for structural and biophysical studies, in particular that of a reduced stability in detergent micelles. Therefore, alternative methods are required for efficient stabilization. Lipid nanodisc made with the membrane scaffold protein MSP is a valuable system but requires a fine optimization of the lipid to protein ratio. We present here the use of the scaffold protein MSP without added lipids as a minimal system to stabilize membrane proteins. We show that this method is applicable to α-helical and β-strands transmembrane proteins. This method allowed cryo-electron microscopy structural study of the bacterial transporter MexB. A protein quantification indicates that MexB is stabilized by two MSP proteins. This simplified and efficient method proposes a new advance in harnessing the MSP potential to stabilize membrane proteins.

1. Introduction

Membrane proteins play key roles in cellular activities and are major targets for medicinal drugs. One hurdle that limits their studies is related to their structural organization. They expose a hydrophobic surface that demands its incorporation into biological membranes. A major challenge for biochemical, biophysical and structural studies, is maintaining membrane proteins in a lipid-like environment for keeping them stable and monodisperse in solution. In order to maintain membrane protein integrity, various solutions for mimicking native lipid-bilayer environments have been described.

Scaffolding systems form a belt around the hydrophobic part of the membrane protein and unlike liposomes, these systems can stabilize membrane proteins as nanometer-size single particles. Scaffolding systems are based on polymers, peptides and proteins. Amphiphilic polymers (Amphipol and SMA) have been developed to stabilize the proteins after detergent exchange and to extract the proteins directly from their native lipid membrane [1,2]. Engineered amphipathic helices and β-sheet peptides are relatively efficient to form lipid nanodisc or to stabilize membrane proteins but present solubility and stability issues [3–5]. Lipoprotein such as apolipoprotein or saposin is potential scaffold proteins to form lipid nanoparticles after detergent removal [6,7]. Proteins in lipid nanoparticles, based on apolipoproteins ApoA1, also termed nanodiscs [8], have been used frequently for biochemical and biophysical studies of membrane proteins and have also been applied for structure determination by single-particle cryo-EM [9–12].

The rationale for the reconstitution of the integral membrane proteins into lipid nanodiscs (ND) is based on the use of a membrane scaffold protein and extra lipids forming the lipid bilayer. Upon detergent removal, the membrane proteins are inserted into a lipid bilayer containing NDs whose size is limited by the membrane scaffold protein (MSP) [13] wrapped around the hydrophobic core of the lipids. A major

* Corresponding author at: CBMN, UMR CNRS 5248, Université Bordeaux, Institut National Polytechnique Bordeaux, Allée Geoffroy Saint-Hilaire, 33600 Pessac, France.
E-mail address: o.lambert@cbmn.u-bordeaux.fr (O. Lambert).
[1] Equally contributing first authors.
[2] Equally contributing last authors.

https://doi.org/10.1016/j.bbamem.2019.01.013
Received 21 September 2018; Received in revised form 17 December 2018; Accepted 24 January 2019
Available online 30 January 2019
0005-2736/

difficulty of forming protein-ND is the control of the number of protein molecules per nanodisc. From our previous results, we have observed that this parameter can be tuned by adjusting the lipid to protein ratio but remains tedious to determine because of the system complexity consisting in two proteins that interplay with lipids [14]. Therefore, we explore the formation of a minimal nanodisc without added exogenous lipids.

Here, we present the reconstitution of membrane proteins with the scaffold protein MSP without added extra lipids. We report a methodology to stabilize representatives of β-strand and α-helical transmembrane proteins with MSP as isolated particles amenable to structural EM studies. This minimal method of the nanodisc formation provides a suitable and straightforward approach for structural studies of individual membrane proteins.

2. Methods

2.1. Materials and reagents

1-Palmitoyl-2-oleoyl-*sn*-glycero-3-phosphocholine (POPC) was purchased from Avanti Polar Lipids (USA), sodium cholate hydrate, octyl-β-D-glucopyranoside (OG) and *n*-Dodecyl β-D-maltoside (DDM) were purchased from Sigma-Aldrich. SM2 Bio-beads was obtained from Bio-Rad. Superose 6 3.2/300 and Superdex 200 PC 3.2/30 columns were purchased from GE Healthcare. Cu 300 mesh grids and C-flat grids were obtained from Agar Scientific and Protochips respectively.

2.2. Lipid preparation

POPC lipids were dissolved in chloroform, dried onto a glass tube under steady flow of nitrogen and followed by exposure to vacuum for 1 h. The lipid film was suspended in the reconstitution buffer (100 mM NaCl, 10 mM Tris/HCl, pH 7.4 (Buffer 1)) and subjected to five rounds of sonication for 30 s each. Lipid concentration was quantified by phosphate analysis.

2.3. Protein preparation

Two membrane scaffold proteins, MSP1D1 and MSP1E3D1 (genetic constructs available from AddGene) were expressed and purified from bacteria [13]. MexB and OprM membrane proteins were expressed and purified from bacteria as previously described for MexB [15], and OprM [16,17]. After purification, protein buffers contained 0.03% *n*-Dodecyl β-D-maltoside for MexB and 0.9% n-octyl-β-D-glucopyranoside for OprM.

2.4. MSP histidine tag cleavage

The linker connecting the histidine tag to the MSP protein contains a recognition site for the AcTEV protease enzyme. Digestion of 1 mg of MSP1E3D1 was performed by incubation with 500 U of AcTEV (Invitrogen) at room temperature for 5 h, following the manufacturer's protocol. The tag-less protein was obtained in the flow through fraction after passage on a Ni-NTA agarose resin (Invitrogen).

2.5. Preparation and purification of MexB-ND, MexB-MSP, OprM-ND and OprM-MSP

MexB was inserted into NDs according to the standard protocol [13,14]. Briefly, to obtain MexB-ND, MexB was mixed with POPC and MSP1E3D1 with or without its His-tag, at a final 32:1:0.5 lipid:MSP:-protein molar ratio in a 10 mM Tris/HCl pH 7.4, 100 mM NaCl buffer with 0.03% DDM and 15 mM Na-cholate (Buffer 2). Unless stated otherwise, molar ratios are calculated based on the monomeric forms of the proteins considered. Detergent was removed by the addition of SM2 Bio-beads into the mixture shaken overnight at 4 °C. MexB-MSP was obtained following the same protocol without addition of POPC. Samples were then purified by size exclusion chromatography (SEC) on a Superose 6 column at 40 μL/min in buffer 1 or by affinity chromatography using a Ni-NTA agarose resin. In the latter case, elution in 10 mM Tris/HCl pH 7.4, 500 mM Imidazole was performed after extensive washing (10CV) to remove excess MSP. Imidazole was then removed by buffer exchange with 10 mM Tris/HCl pH 7.4, 100 mM NaCl on an amicon ultra 100,000 MWCO by 5 centrifugations at 3000*g* for 10 min.

For OprM-ND, OprM was mixed with POPC and MSP1D1 at a final 24:1:0.6 lipid:MSP:protein molar ratio in a 10 mM Tris/HCl pH 7.4, 100 mM NaCl buffer with 0.9% β-octylglucoside and 15 mM Na-cholate (Buffer 3). Detergent was removed by SM2 Bio-beads overnight at 4 °C. OprM-MSP was reconstituted following the same protocol, without addition of lipids. Samples were then purified by SEC on a Superose 6 column at 40 μL/min in buffer 1.

An alternative reconstitution of OprM-MSP and MexB-MSP was performed on spin columns. For OprM-MSP, OprM was mixed with MSP1D1 at a final 1:0.6 MSP:protein molar ratio in buffer 3 and incubated with slight agitation for 1 h at 4 °C. For MexB-MSP, MexB was mixed with MSP1D1 at a final 1:0.5 MSP:protein molar ratio in buffer 2 and incubated with slight agitation for 1 h at 4 °C. Equilibration of zeba spin desalting columns (MWCO 7 K, Thermo Fisher) was achieved by three centrifugations with 300 μL of buffer 1 at 2000*g* for 1 min. Then, the reconstitution mixture was applied onto the column and the complex was collected in the flow through after centrifugation for 2 min at 2000*g*.

2.6. Protein quantification from SDS polyacrylamide gel electrophoresis (SDS-PAGE)

Protein samples were boiled for 10 min at 100 °C in 1× SDS-PAGE reducing buffer and ran for 1 h at a constant voltage of 180 V on a 12% polyacrylamide gel following the protocol of Laemmli [18]. Protein bands were stained by overnight incubation in SYPRO ruby gel stain solution (Bio-Rad) with slow agitation. Excess background staining was removed by two successive 30 min incubations in a solution containing 10% methanol and 7% acetic acid. The gels were washed one last time in ultrapure water and imaged on a Typhoon 8600 (Molecular dynamics) in fluorescence mode using a green excitation laser (λ = 532 nm) and the Rox 610 BP 30 emission filter at a normal sensitivity.

The quantification of protein bands was achieved using the gel analyzer plugin of the imageJ software for integration of the area under the peaks. Construction of a standard curve using BSA allowed the determination of the samples protein content in micrograms. The corresponding number of moles for each protein was calculated as follows:

$$n_{(MexB)} = \mu g_{(MexB)} \times 10^{-6} \times F_{(MexB)}/MW_{(MexB)} \text{ and } n_{(MSP1E3D1)} = \mu g_{(MSP1E3D1)} \times 10^{-6} \times F_{(MSP1E3D1)}/MW_{(MSP1E3D1)}$$

where $F_{(MexB)}$ and $F_{(MSP1E3D1)}$ are correction factors equal to 0.8 and 1.3 respectively calculated from the ratio of the slopes (s) for the standard curves of MexB, BSA and MSP1E3D1 ($F_{(MexB)} = s_{(BSA)} / s_{(MexB)} = 0.8$; $F_{(MSP1E3D1)} = s_{(BSA)} / s_{(MSPE31D1)} = 1.3$). Finally, in order to account for the trimeric nature of MexB, we multiplied by 3 the molar ratio of MSP to MexB.

2.7. Lipid content characterized by attenuated total reflection Fourier transform infrared spectroscopy (ATR-FTIR)

Polarized ATR-FTIR spectra were recorded on a Nicolet 6700 FT-IR spectrometer (Nicolet Instrument) with a spectral resolution of 4 cm^{-1}. MexB samples at 0.5 mg/mL were deposited on the crystal in a 10 μL droplet. The surface was washed twice with Tris/HCl 10 mM pH 7.4, 100 mM NaCl and the spectra of the adsorbed molecules were recorded

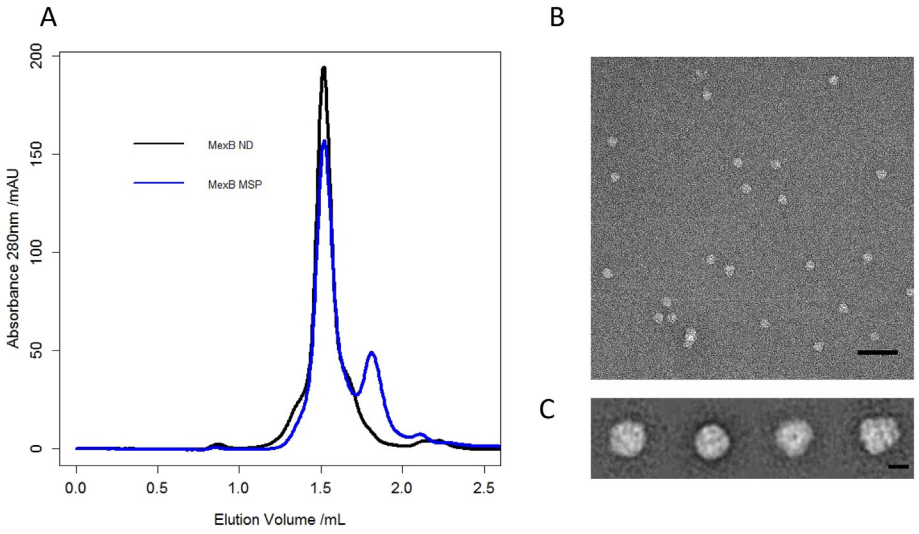

Fig. 1. A) Size Exclusion Chromatography elution profiles for MexB-MSP (blue curve) and MexB reconstituted in lipid nanodisc using the same MSP1E3D1 (MexB-ND). For MexB-MSP, an extra peak is observed at 1.8 mL eluted volume, indicating an excess of free MSP. B) Negative stain EM field of the peak at 1.5 mL eluted volume showing homogeneous MexB-MSP particles. Scale bar 50 nm. C) Representative 2D classes of MexB viewed with different orientations. The two average images on the right correspond to top and side views respectively. Scale bars 10 nm. (For interpretation of the references to color in this figure legend, the reader is referred to the web version of this article.)

with a parallel (p) and perpendicular (s) polarization of the incident light. The observation of characteristic absorption bands for protein and lipid molecules and comparison of their relative intensities across the different samples allowed for the assessment of lipid content for each specimen.

2.8. Negative stain electron microscopy

For EM grid preparation, a diluted mixture of MexB-MSP (at 0.005 mg/mL) or OprM-MSP (at 0.01 mg/mL) samples was applied to a glow-discharged carbon-coated copper 300 mesh grid and stained with 2% uranyl acetate (w/v) solution. Images were recorded under low dose conditions on F20 electron microscope operated at 200 kV using a Eagle 4 k × 4 k camera (FEI). 1902 and 2413 particles were manually picked from 300 and 50 micrographs for MexB and OprM respectively, and image alignment and two-dimensional averages were performed using Eman2.

2.9. Single particle cryo-electron microscopy

MexB-MSP was characterized in a second time by single particle analysis in cryo-electron microscopy. Holey carbon grids (300mesh R2/1 C-Flat) were treated with a glow discharge before a deposition of a 3 µL aliquot at 4 mg/mL for 1 min. The grid was blotted for 1 s (Whatmann paper ashless 42), rapidly plunged and frozen in liquid ethane using EMGP (Leica) with 5 °C controlled temperature and 60% regulated hygrometry. The grids were stored in liquid nitrogen before grid checking and imaging. The data collection of MexB-MSP was carried out automatically on a Polara (FEI) operated at 300 kV using K2 Summit direct electron detector (GATAN). A data set of 445 dose fractionated micrographs was recorded in counting mode with a pixel size of 1.21 Å. Each micrograph was collected as 40 movie frames of 0.15 s with a dose rate of 1 e^{-} $Å^{-2}$ s^{-1} each. The total dose was about 40 e^{-} $Å^{-2}$. Images were recorded using the automated acquisition program Latitude S from Gatan with defocus values ranging from −1.5 to −3 µm.

All movie frames were corrected for gain reference and aligned using Motioncorr2 [19]. Contrast transfer function (CTF) parameters were estimated using Gctf [20]. Further image processing was done in RELION2.1. Initial particle picking consists in a manual-picking of 1181 particles to calculate 2D references. These 2D templates were low-pass filtered to 20 Å to limit reference bias and used for automated picking of all micrographs. A total of 50,722 particles from 233 micrographs were picked. After a 2D classification, 50,522 particles were selected for further analyses. A particle subset was used to calculate a 60 Å low-pass filtered initial model. The 50,522 particles were subjected to 3D classification into 10 classes with no symmetry imposed. Four classes, exhibiting similar structural features and comprising a total of 24,576 particles were subjected to 3D refinements with C1 symmetry. Since MexB has been described as an asymmetric homotrimer, no symmetry was imposed. The resolution estimation calculated onto two separately 3D refined half-reconstructions with the Fourier shell correlation criterion at 0.143 was 8.4 Å for C1 symmetry reconstruction.

3. Results

3.1. Stabilization of a α-helical transmembrane protein with MSP scaffold protein

We evaluated the ability of MSP1E3D1 to stabilize, in a detergent-free buffer, the MexB drug transporter, as a representative of α-helical transmembrane protein. In Gram-negative bacteria, MexB forms an asymmetric trimer in which each protomer is made of a 12 transmembrane α-helices domain and a large periplasmic part comprising a porter and a funnel domain extending 7 nm away from the inner membrane inside the periplasm. We incubated the detergent-purified MexB protein with MSP1E3D1 at a MSP:MexB molar ratio of 2:1 and then proceeded to the detergent removal with Bio-beads. The sample was thereafter submitted to SEC using a buffer without detergent (buffer 1). The SEC profile showed two peaks; the first peak corresponds to the MexB stabilized with MSP (MexB-MSP) whereas the second peak originates from monomeric MSP (Fig. 1A). For comparison, a solution of MexB stabilized in a lipid nanodisc (MexB-ND) submitted to SEC exhibited a comparable elution profile suggesting that MexB-MSP and MexB-ND have similar sizes with Superose 6 column. Note that when SEC was performed with a Superdex 200 column, the elution peak for MexB-MSP is slightly shifted toward the right indicative of a smaller size compared with MexB-ND containing additional lipids (Fig. S1 Supplementary materials).

EM revealed a homogenous population of MexB-MSP molecules (Fig. 1B). Averaging 1902 single particles showed side and top views of MexB-MSP in accordance with the trimeric organization of MexB (PDB ID: 2V50) with a continuous layer of electron density for the MSP, including the 36-transmembrane helix domain of trimeric MexB. Furthermore, the periplasmic part of MexB exhibited two clearly distinguishable layers of density, assigned to the porter domain and to the more distal funnel domain (Fig. 1C).

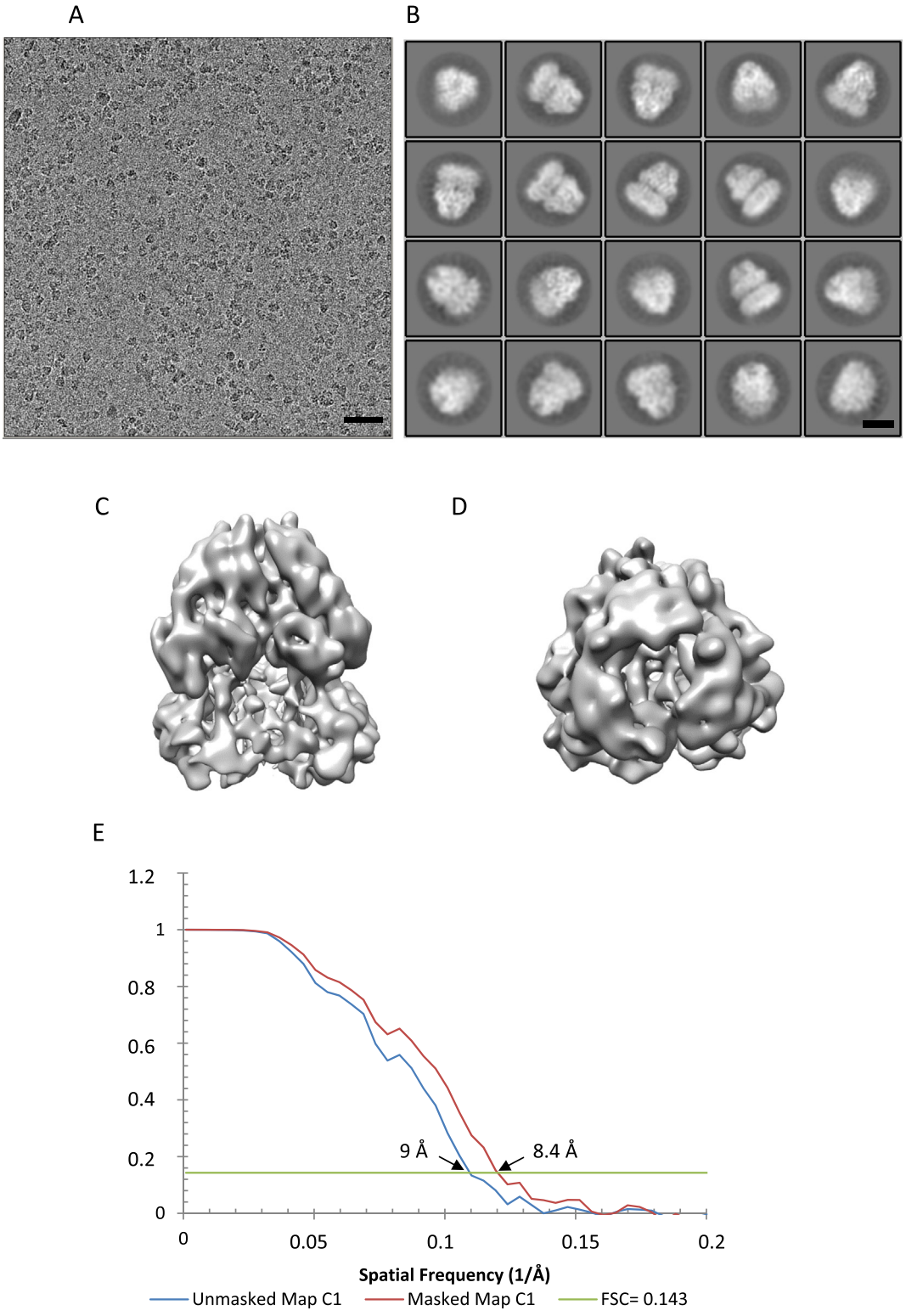

Fig. 2. Cryo-EM data and image processing of MexB-MSPE3D1. A) Representative cryo-EM micrograph. Scale bar 50 nm. B) Average images after 2D classification. Scale bar 7 nm. C–D) Side and top views of MexB-MSP cryo-EM reconstruction. E) Resolution curve.

3.2. Single particle cryo-electron microscopy of MexB-MSP

We used single-particle cryo-EM to determine the structure of MexB-MSP. We prepared cryo-EM grids of the MexB-MSP by the standard plunge-freezing method. Cryo-EM images showed that the frozen hydrated complexes of MexB-MSP were homogeneous and monodisperse (Fig. 2A). We collected a relatively modest cryo-EM data set (455 micrographs) as the purpose of this structural study was conceived as a proof of feasibility but not as the elucidation of MexB structure, which is already known [21]. The 2D class averages displayed thin features of the periplasmic and transmembrane domains of MexB-MSP viewed in various orientations (Fig. 2B). After 3D classification, four classes

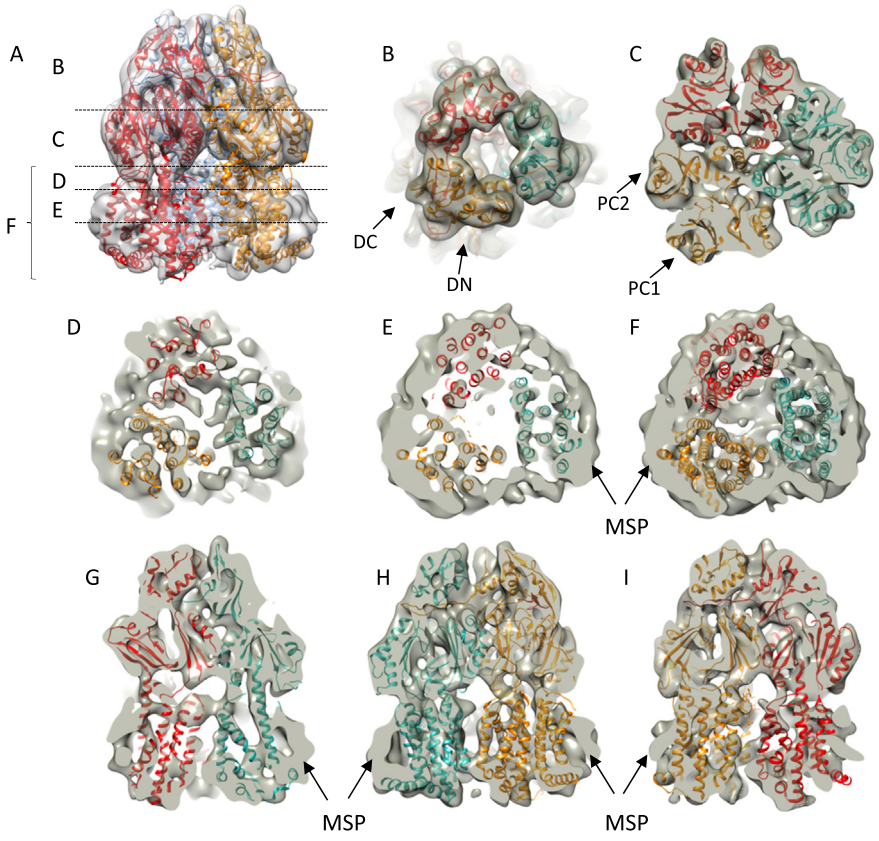

Fig. 3. Fitting of MexB crystal structure within the cryo-EM map.
A) Side view of MexB in the cryo-EM map B–F) Transversal sections through the volume showing the fit of each asymmetric subunit colored in red, yellow and blue corresponding to the Access, Binding and Extrusion conformation respectively. Selected position at the level of the funnel domain (B), porter domain (C), transmembrane domain (D-F) marked on A). G-I) Longitudinal sections revealing good fit of transmembrane helices of blue and yellow subunits corresponding to Binding and Extrusion conformations. (For interpretation of the references to color in this figure legend, the reader is referred to the web version of this article.)

comprising a total of 24,576 particles were used to calculate a 3D reconstruction following a gold-standard refinement procedure at a resolution of 8.4 Å (estimated with the criterion of Fourier shell correlation FSC = 0.143) (Figs. 2C, D, E). The Euler angle distribution showed a good spatial coverage of all particles used in the final map (Fig. S2 Supplementary materials). No symmetry was imposed as MexB forms an asymmetric homotrimer [21].

Surface representations of MexB-MSP cryo-EM densities show that the periplasmic core of MexB was better resolved than some domains at the edge of the molecule that seem highly flexible as well as the region that could be attributed to the MSP proteins (Fig. 2D–C). The asymmetric MexB crystal structure could be directly fitted within our cryo-EM map without modification. Overall no significant difference was observed between the two structures (Fig. 3). The three asymmetric subunits (in Access, Binding and Extrusion conformations) as described in the crystal structure [21,22] have been positioned in the C1 cryo-EM map. The secondary structure elements could be assigned within the periplasmic domain which confirms the 8.4 Å resolution. The funnel domains DN and DC were well-accommodated and the α-helices and loops were clearly defined (Fig. 3B) as well as the porter domains PC1 and PC2 (Fig. 3C). Transmembrane densities exhibited a good fit with transmembrane helices of the Binding and Extrusion subunits from the crystal structure unlike densities corresponding to those of the Access subunit (Fig. 3E, G–I). For the latter, the bundle of helices in the EM map was resolved but a small shift was observed with respect to the helices from the crystal. This structural variation may likely be explained by the use of MSP instead of detergent. Such mobility of the helices was already observed when AcrB, *E. coli* transporter homologous to MexB was solubilized with SMA [23], suggesting the position of the transmembrane helices are slightly modified by the presence of the stabilizing molecules. In addition, extra densities around MexB could correspond to the MSP molecules but poor resolution did not permit to solve the MSP structure (Fig. 3E–I). Overall, the C1 cryo-EM map was in good agreement with the crystal structure and the stabilization with MSP did not induce major changes to the global secondary structure in MexB.

3.3. Analysis of MexB-MSP stoichiometry

To determine the stoichiometry of MSP bound per MexB trimer within the MexB-MSP complex, we reconstituted MexB-MSP1E3D1 with a MSP devoid of its His-tag and removed the excess of MSP by affinity purification using the His-tag of MexB. SDS-PAGE of purified MexB-MSP with BSA-standards as a reference (Fig. 4) suggested a 2:1 ratio of MSP/MexB trimer (Table 1).

In this range of concentration, the fluorescence intensities of MexB and MSP1E3D1 were proportional to the amount of protein but differed slightly from the BSA-standards at similar concentrations (Fig. S3A Supplementary materials). To get an accurate quantification from the BSA standard curve, an adjustment factor using the ratio of their slopes has been applied as described in Materials and Methods (Fig. S3B Supplementary materials). For comparison, a MexB-ND sample prepared in a way similar to that of MexB-MSP showed a comparable stoichiometry suggesting that there are two MSP molecules in both MexB-MSP and MexB-ND complexes (Table 1).

3.4. Characterization of lipid content of MexB-ND and MexB-MSP by ATR-FITR

Given that membrane proteins after purification with detergent may conserve some lipid molecules tightly bound to their transmembrane regions, we sought to evaluate if a large amount of residual lipids could be responsible for MexB stabilization by MSP. To this end, reconstitution of MexB-ND2 was performed with a lipid concentration two fold larger than that of MexB-ND, for a characterization of the lipid content using polarized ATR-FTIR. ATR spectra were collected for MexB-MSP, MexB-ND and MexB-ND2 between 4000 cm^{-1} and 600 cm^{-1}. The presence of lipid was detected by following the absorption bands

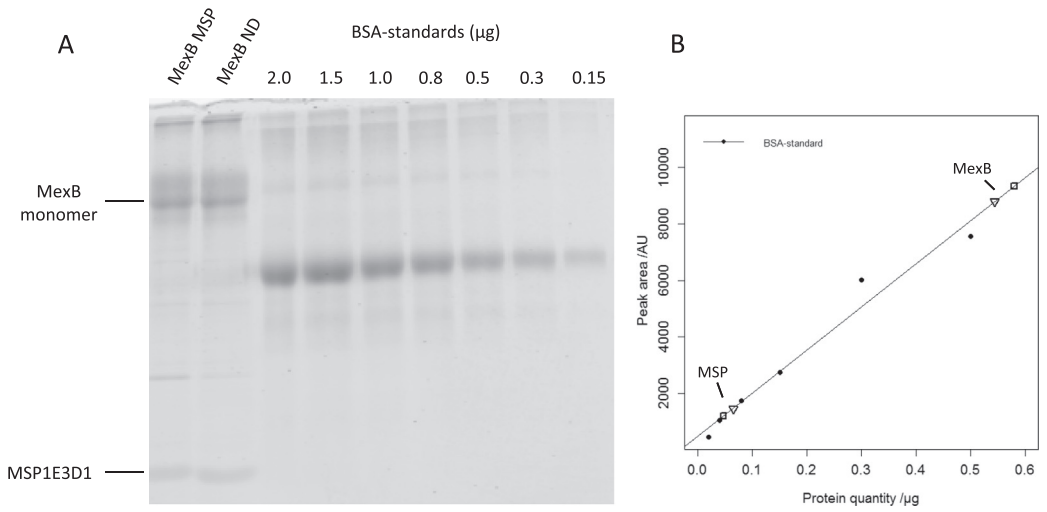

Fig. 4. Determination of the molar MSP to MexB ratio by SYPRO ruby quantification.
A) SDS PAGE of MexB-MSP, MexB-ND and BSA-standards. The samples were run on the same gel as the BSA-standards to ensure proper calibration. B) Protein quantities for MexB and MSP1E3D1 were determined for both MexB-ND (triangles) and MexB-MSP (squares) complexes by use of the BSA calibration curve.

Table 1
MSP to MexB molar ratio. Values presented are the average of two independent experiments.

	MSP to MexB molar ratio	
	Mean	SD
MexB ND	1.7	0.3
MexB MSP	1.5	0.2

around 2923 cm^{-1} and 2850 cm^{-1} which correspond to the antisymmetric and symmetric CH_2 stretching modes of the lipid acyl chains respectively (Fig. 5). The intensities of the absorption bands are proportional to the molecule concentration and these increased with increasing lipid to protein ratio used for MexB-ND reconstitution. Indeed, a doubling of the lipid to protein ratio resulted in twice as much signal in the CH_2 region, going from $2.3.10^{-4}$ to $4.5.10^{-4}$ at 2920 cm^{-1} and from $1.0.10^{-4}$ to 2.10^{-4} at 2850 cm^{-1} for the MexB-ND and MexB-ND2 samples respectively. The presence of amide bands between 1600–1700 (amide I) and 1500–1580 (amide II) clearly demonstrates the presence of the proteins. For all studied samples, comparable intensities were observed, indicating that similar quantities of MexB-ND2 or MexB-ND were adsorbed on the crystal providing further evidence that the difference in signal for the bands at 2923 cm^{-1} and 2850 cm^{-1} was due to different lipid concentrations. Specifically, in the vicinity of the wavenumbers where a lipid contribution should appear, MexB-MSP exhibited only background level absorbance intensity revealing the absence of endogenous lipids surrounding its transmembrane region. Interestingly, when more lipids were used for nanodisc reconstitution, i.e. for MexB-ND2, a characteristic band of the ester carbonyl stretching mode appeared at 1740 cm^{-1} which unequivocally identified the presence of lipids. In conclusion, the MexB-MSP complex was stabilized mainly by direct protein-protein contacts and no significant amounts of leftover lipids were required to accommodate interactions between

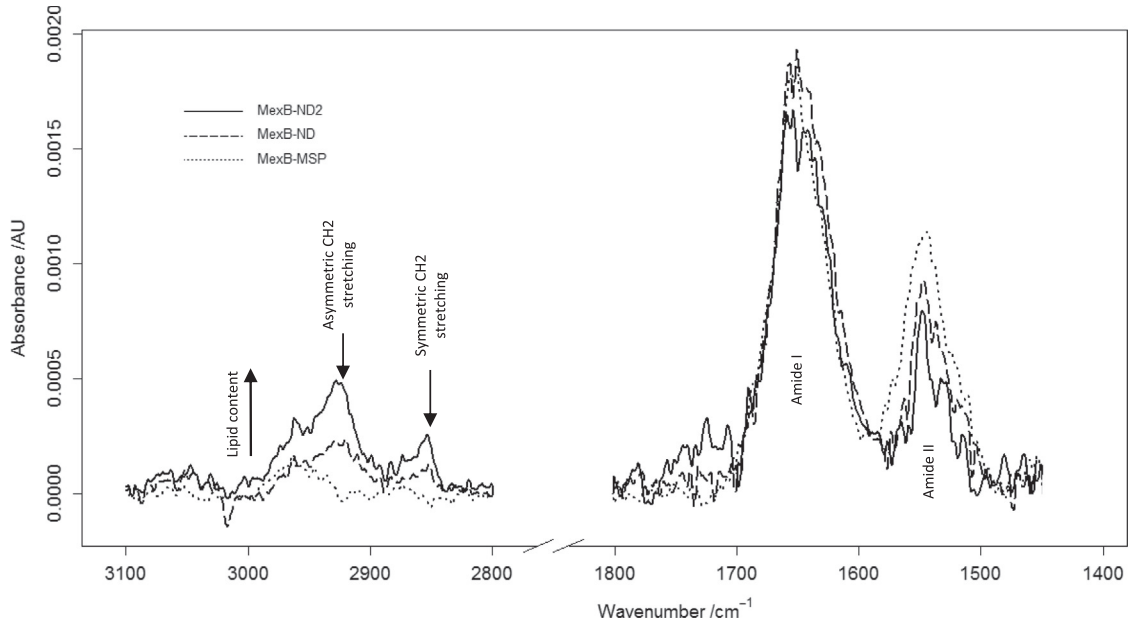

Fig. 5. ATR-FITR characterization of lipid content for MexB reconstituted in ND or with MSP alone.
ATR-FTIR *p*-polarized spectra show the presence of lipids for MexB-ND according to the absorption bands at 2923 cm^{-1} and 2850 cm^{-1} (arrows). Doubling the lipid to protein ratio for MexB-ND reconstitution (MexB-ND2) results in a two-fold increase in the concentration of lipids per nanodisc, as shown by the MexB-ND2/MexB-ND ratio in the CH_2 bands intensity, while the amount of protein adsorbed remains constant as indicated by the intensity of the amide bands (between 1600–1700 cm^{-1} (amide I) and 1500–1580 cm^{-1} (amide II). Unlike MexB-ND, the MexB-MSP spectrum shows undetectable amount of endogenous lipids.

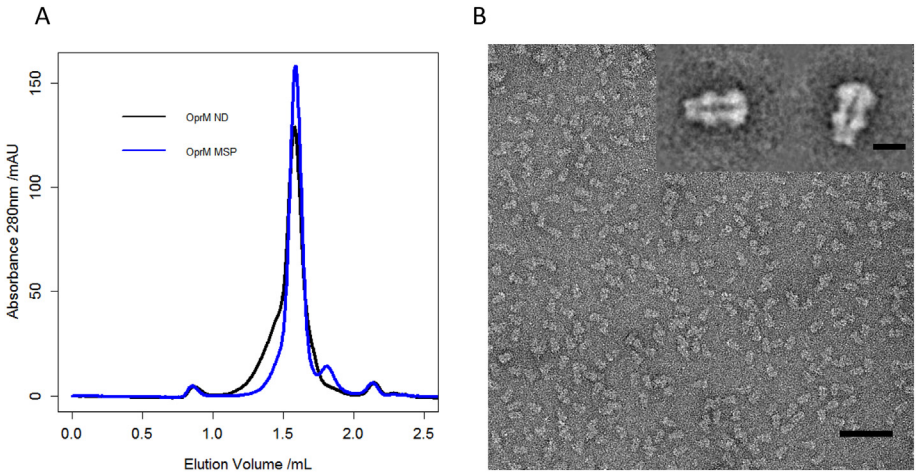

Fig. 6. A) Size Exclusion Chromatography elution profiles for OprM-ND and OprM-MSP. In the latter case, an extra peak is observed, indicating an excess of free MSP. Higher molecular weight species are present in the OprM ND reconstitution. B) EM observation of the OprM-MSP fraction shows isolated OprM molecules. Scale bar 50 nm. Inset: representative class average of OprM negatively stained images. Scale bar 7 nm.

MexB and its MSP.

To get further information on the amount of lipids associated with the MexB-ND, a gas chromatography equipped with flame-ionization detection (GC-FID) has been carried out on MexB-ND (Fig. S4 and Table S1 Supplementary materials). The lipid to protein ratio (mol/mol) was estimated to be 39 that corresponds to about 117 lipid molecules per nanodisc that is compatible with lipid content estimated in MSP1E3D1 nanodisc [13].

3.5. Stabilization of a β-strand transmembrane protein with MSP scaffold protein

To further determine whether a membrane protein with a smaller transmembrane domain could be stabilized by a MSP alone, we focused on the potential of MSP1D1 to stabilize OprM which possesses a trimeric organization consisting in a β-barrel transmembrane domain of 4–5 nm in diameter. We incubated the detergent-purified OprM protein with MSP1D1 at a MSP:OprM molar ratio of 1:0.6 and then proceeded to remove the detergent with Bio-beads. The SEC profile showed a main peak corresponding to the OprM stabilized with MSP (OprM-MSP) (Fig. 6A). OprM reconstituted in lipid nanodisc (OprM-ND) showed a comparable elution profile that appeared thicker than that of OprM-MSP suggesting a higher homogeneity for OprM-MSP. EM analysis of these OprM-MSPs revealed a homogenous population of OprM-MSP molecules with their long axis preferentially oriented parallel to the carbon support which was consistent with the trimeric assembly of OprM (Fig. 6B) [24,25]. An average image (from 2413 particles) of OprM-MSP revealed densities related to the MSP at the edge of the duct formed by the OprM β-barrel domain and the 10-nm-long OprM periplasmic domain (Fig. 6B, inset). A previous EM characterization of OprM-ND showed also one trimer per ND [14]. Of note, the ND size appeared slightly larger because of the presence of lipids. It appears MSP1D1 without extra lipids also allowed the stabilization of one trimer of OprM.

Our protocol for measuring the OprM/MSP ratio required the removal of the MSP excess using His-tag affinity chromatography and elution of OprM-MSP complexes. Unfortunately, we observed that during this step, a molecular reorganization occurred within these complexes leading to the formation of complexes containing two or three OprM molecules. Therefore, the OprM/MSP ratio has not been determined because the presence of these complexes would have biased the calculation of the number of MSP per OprM trimer. For OprM-ND, the ratio MSP/OprM indicated that one OprM particle is stabilized by two MSP molecules, like MexB-ND and MexB-MSP (data not shown).

4. Discussion

Nanodiscs currently developed for stabilizing membrane protein in detergent-free buffer use scaffold proteins and extra lipids leading to the formation of a tripartite scaffold-lipid-protein complex [9,26,27]. We have explored the ability of the ApoA1-derived MSP protein to stabilize membrane protein in detergent-free buffer without adding extra lipids for structural and biophysical studies. The formation of MSP-membrane protein complex was carried out by detergent removal.

We successfully stabilized representatives of both β-barrel and α-helical membrane proteins with MSP1D1 and MSP1E3D1. We carried out a cryo-EM structure determination of MexB stabilized by MSP indicating that the overall structure of MexB stabilized by MSP resembles the asymmetric crystal structure of MexB in detergent (Fig. 3). Our results also provided evidence that trimeric MexB particles were stabilized by two MSP molecules (Fig. 4). In pure lipid nanodiscs, it has been proposed that two MSP molecules form a double-belt shielding the acyl chains of the lipid molecules [27–29]. Likewise, cryo-EM density map showed extra densities around the transmembrane domain of MexB. The MSP densities were poorly resolved probably because of an irregular arrangement of MSP molecules. However, their disposition strongly suggests that the MSP proteins are wrapped around MexB. Moreover, the similar sizes obtained for pure lipid nanodiscs and MexB-MSP suggest a similar arrangement of the scaffolding protein, in a double belt-like pattern, as previously proposed [29].

The stabilization of OprM has been achieved with MSP1D1. The choice of this MSP was driven by our previous data on the formation of OprM-ND [14]. We had been able to reconstitute OprM in nanodisc using this MSP. Therefore, we used the same MSP to stabilize OprM without extra lipids. The EM results after size exclusion chromatography show a homogeneous distribution of OprM molecules (Fig. 6). These results indicate that the MSP on its own with no extra lipids, is able to maintain the stability and monodispersity of membrane proteins in a detergent-free buffer even for proteins harboring a rather small transmembrane domain (5 nm in diameter for OprM). It can be assumed that MSP molecules adopt an organization that encircles OprM, as for MexB. Given the MSP flexibility revealed by the cryo-EM structure of MexB-MSP, we expect similar variabilities in MSP structural arrangements around OprM which would hamper the determination of its organization by single particle cryo-EM explaining why we did not pursue further cryo-EM structural investigation.

Stabilizing membrane proteins with MSP in the absence of lipids presents several advantages. First, defining the MexB/MSP ratio to get one trimeric MexB particle per complex seems rather straightforward. As long as MSP is present in a little excess, MexB will be well stabilized. In our experiments, we have used a MSP/MexB ratio of 2. There is no need to add a larger excess of MSP. In the case of lipid nanodisc

formation, the addition of lipids may affect the number of MexB protein per ND inducing a certain heterogeneity [30]. This explains why the lipid to protein ratio needs to be finely adjusted to maintain one molecule of MexB per ND. Secondly, the method for removing detergent classically uses polystyrene beads. Another method has also been explored with the use of spin column. The advantage of this method is a much quicker detergent removal than with the Bio-beads. The stabilization of OprM and MexB has been performed with the MSP1D1 and the samples were observed by electron microscopy (Fig. S5 Supplementary materials). Both OprM and MexB samples looked homogeneous and similar to those prepared with Bio-beads. For the formation of lipid nanodisc, the rate of detergent removal is important for the bilayer reconstitution. Altogether, the stabilization of membrane proteins with MSP in the absence of additional lipids appears less restrictive.

The ability of scaffolding systems to stabilize membrane proteins without adding extra lipids has been proposed for engineered peptides forming β-strands and α-helices. Such stabilization was successful for the MsbA transporter, rhodopsin and bacteriorhodopsin that are α-helical integral membrane proteins but failed for the β-barrel PhoE porin [3,4]. Very recently a bi-helical peptide has been developed with the ability to stabilize both α-helical and β-barrel membrane proteins [31]. Our results extend this approach to the use of proteins such as MSP containing several helical segments without the need for peptide engineering.

The use of a minimal system like MSP for stabilizing membrane proteins offers several practical advantages. Their preparation is fast and easier since there is no need to optimize the lipid to protein ratio that can be tedious. According to our results, this minimal MSP nanodisc provides a suitable environment for structural study using single particle cryoEM. Although limited, the minimal MSP may offer some interest for studying particular aspects of the lipid environment on the membrane protein function. Since the protein is already stabilized by the MSP, the effect of a particular lipid such as cholesterol or non-bilayer forming lipid could be analyzed without the need of extra bilayer forming lipids.

Even though our cryo-EM structure of MexB-MSP revealed the asymmetric structure of MexB encircled by densities attributable to the MSP, it did not permit to describe the interactions of MSP with MexB. Nevertheless, these densities were located in the close vicinity of MexB suggesting a direct interaction of MSP with MexB. This hypothesis is supported by ATR-FTIR results showing no detectable lipid content associated with MexB (Fig. 5), although it cannot be excluded that a few lipids remained strongly bound the membrane protein after its purification and may help its stabilization with the scaffolding protein.

5. Conclusions

Our protocol opens the use of MSP for stabilizing membrane protein without adding extra lipids. This method is less restrictive than that for preparing lipid nanodisc in terms of MSP to protein ratio optimization, detergent removal or even the choice of MSP length. Membrane proteins are well maintained as isolated particles amenable to single particle cryo-EM structural studies. As a scaffold protein, the same MSP can be used with or without extra lipids for stabilizing membrane proteins. This versatile property may emerge as a valuable advantage to use a unique scaffold system instead of several for biochemical, structural and pharmacological characterizations.

Transparency document

The Transparency document associated with this article can be found, in online version.

Acknowledgments

This work was supported by French national agency ANR (Assembly ANR-17CE11-0028), Bordeaux INP and Conseil Régional Aquitaine. This work has benefited from the facilities of UMS3033/US001 (http://www.iecb.u-bordeaux.fr/index.php/fr/plateformestechnologiques), the Bordeaux Metabolome Facility-MetaboHUB (grant no. ANR–11–INBS–0010) and used the platforms of the Grenoble Instruct-ERIC Center (ISBG: UMS 3518 CNRS-CEA-UGA-EMBL) with support from FRISBI (ANR-10 INSB-05-02) and GRAL (ANR-10-LABX-49-01) within the Grenoble Partnership for Structural Biology (PSB). The electron microscope facility is supported by the Rhône-Alpes Region, the Fondation Recherche Medicale (FRM), the Fonds Européen de Développement Régional (FEDER) and the GIS-Infrastructures en Biologie Sante et Agronomie (IBISA). DS is recipient of a MENRT fellowship. MG is recipient of a fellowship from Bordeaux-INP and Conseil Régional d'Aquitaine. We thank C. Gounou for technical assistance. We acknowledge the platform Metabolome-Fluxome-Lipidome of Bordeaux (http://www.biomemb.cnrs.fr/INDEX.html) for contribution to lipid analysis.

Author contributions

OL, LD, DS, MG designed the project, analysed data and wrote the manuscript. DS, MG, GS carried out experiments. IB, GP, CG developed expression and protein purification protocols. SL advised on ATER experiment. MD, JCT assisted with electron microscopy and image analysis. SM performed lipid analysis.

Competing financial interests

The authors declare no competing financial interests.

Appendix A. Supplementary data

Supplementary data to this article can be found online at https://doi.org/10.1016/j.bbamem.2019.01.013.

References

[1] C. Tribet, R. Audebert, J.L. Popot, Amphipols: polymers that keep membrane proteins soluble in aqueous solutions, Proc. Natl. Acad. Sci. U. S. A. 93 (1996) 15047–15050.
[2] T.J. Knowles, R. Finka, C. Smith, Y.-P. Lin, T. Dafforn, M. Overduin, Membrane proteins solubilized intact in lipid containing nanoparticles bounded by styrene maleic acid copolymer, J. Am. Chem. Soc. 131 (2009) 7484–7485, https://doi.org/10.1021/ja810046q.
[3] C.E. Schafmeister, L.J. Miercke, R.M. Stroud, Structure at 2.5 A of a designed peptide that maintains solubility of membrane proteins, Science 262 (1993) 734–738.
[4] H. Tao, S.C. Lee, A. Moeller, R.S. Roy, F.Y. Siu, J. Zimmermann, R.C. Stevens, C.S. Potter, B. Carragher, Q. Zhang, Engineered nanostructured β-sheet peptides protect membrane proteins, Nat. Methods 10 (2013) 759–761, https://doi.org/10.1038/nmeth.2533.
[5] A.N. Larsen, K.K. Sørensen, N.T. Johansen, A. Martel, J.J.K. Kirkensgaard, K.J. Jensen, L. Arleth, S.R. Midtgaard, Dimeric peptides with three different linkers self-assemble with phospholipids to form peptide nanodiscs that stabilize membrane proteins, Soft Matter 12 (2016) 5937–5949, https://doi.org/10.1039/c6sm00495d.
[6] T.H. Bayburt, J.W. Carlson, S.G. Sligar, Reconstitution and imaging of a membrane protein in a nanometer-size phospholipid bilayer, J. Struct. Biol. 123 (1998) 37–44, https://doi.org/10.1006/jsbi.1998.4007.
[7] J. Frauenfeld, R. Löving, J.-P. Armache, A.F.-P. Sonnen, F. Guettou, P. Moberg, L. Zhu, C. Jegerschöld, A. Flayhan, J.A.G. Briggs, H. Garoff, C. Löw, Y. Cheng, P. Nordlund, A saposin-lipoprotein nanoparticle system for membrane proteins, Nat. Methods 13 (2016) 345–351, https://doi.org/10.1038/nmeth.3801.
[8] T.H. Bayburt, Y.V. Grinkova, S.G. Sligar, Assembly of single bacteriorhodopsin trimers in bilayer nanodiscs, Arch. Biochem. Biophys. 450 (2006) 215–222, https://doi.org/10.1016/j.abb.2006.03.013.
[9] J. Frauenfeld, J. Gumbart, E.O. van der Sluis, S. Funes, M. Gartmann, B. Beatrix, T. Mielke, O. Berninghausen, T. Becker, K. Schulten, R. Beckmann, Cryo-EM structure of the ribosome-SecYE complex in the membrane environment, Nat. Struct. Mol. Biol. 18 (2011) 614–621, https://doi.org/10.1038/nsmb.2026.

[10] R.G. Efremov, A. Leitner, R. Aebersold, S. Raunser, Architecture and conformational switch mechanism of the ryanodine receptor, Nature 517 (2015) 39–43, https://doi.org/10.1038/nature13916.
[11] Y. Gao, E. Cao, D. Julius, Y. Cheng, TRPV1 structures in nanodiscs reveal mechanisms of ligand and lipid action, Nature 534 (2016) 347–351, https://doi.org/10.1038/nature17964.
[12] P. Jin, D. Bulkley, Y. Guo, W. Zhang, Z. Guo, W. Huynh, S. Wu, S. Meltzer, T. Cheng, L.Y. Jan, Y.-N. Jan, Y. Cheng, Electron cryo-microscopy structure of the mechanotransduction channel NOMPC, Nature 547 (2017) 118–122, https://doi.org/10.1038/nature22981.
[13] T.K. Ritchie, Y.V. Grinkova, T.H. Bayburt, I.G. Denisov, J.K. Zolnerciks, W.M. Atkins, S.G. Sligar, Chapter 11 - reconstitution of membrane proteins in phospholipid bilayer nanodiscs, Methods Enzymol. 464 (2009) 211–231, https://doi.org/10.1016/S0076-6879(09)64011-8.
[14] L. Daury, F. Orange, J.-C. Taveau, A. Verchère, L. Monlezun, C. Gounou, R.K.R. Marreddy, M. Picard, I. Broutin, K.M. Pos, O. Lambert, Tripartite assembly of RND multidrug efflux pumps, Nat. Commun. 7 (2016) 10731, , https://doi.org/10.1038/ncomms10731.
[15] V. Mokhonov, E. Mokhonova, E. Yoshihara, R. Masui, M. Sakai, H. Akama, T. Nakae, Multidrug transporter MexB of Pseudomonas aeruginosa: overexpression, purification, and initial structural characterization, Protein Expr. Purif. 40 (2005) 91–100, https://doi.org/10.1016/j.pep.2004.10.002.
[16] Y. Ferrandez, M. Dezi, M. Bosco, A. Urvoas, M. Valerio-Lepiniec, C. Le Bon, F. Giusti, I. Broutin, G. Durand, A. Polidori, J.-L. Popot, M. Picard, P. Minard, Amphipol-mediated screening of molecular orthoses specific for membrane protein targets, J. Membr. Biol. 247 (2014) 925–940, https://doi.org/10.1007/s00232-014-9707-3.
[17] G. Phan, H. Benabdelhak, M.-B. Lascombe, P. Benas, S. Rety, M. Picard, A. Ducruix, C. Etchebest, I. Broutin, Structural and dynamical insights into the opening mechanism of *P. aeruginosa* OprM channel, Struct. Lond. Engl. 1993 (18) (2010) 507–517, https://doi.org/10.1016/j.str.2010.01.018.
[18] U.K. Laemmli, Cleavage of structural proteins during the assembly of the head of bacteriophage T4, Nature 227 (1970) 680–685.
[19] X. Li, P. Mooney, S. Zheng, C. Booth, M.B. Braunfeld, S. Gubbens, D.A. Agard, Y. Cheng, Electron counting and beam-induced motion correction enable near atomic resolution single particle cryoEM, Nat. Methods 10 (2013) 584–590, https://doi.org/10.1038/nmeth.2472.
[20] K. Zhang, Gctf: real-time CTF determination and correction, J. Struct. Biol. 193 (2016) 1–12, https://doi.org/10.1016/j.jsb.2015.11.003.
[21] G. Sennhauser, M.A. Bukowska, C. Briand, M.G. Grütter, Crystal structure of the multidrug exporter MexB from Pseudomonas aeruginosa, J. Mol. Biol. 389 (2009) 134–145, https://doi.org/10.1016/j.jmb.2009.04.001.
[22] R. Nakashima, K. Sakurai, S. Yamasaki, K. Hayashi, C. Nagata, K. Hoshino, Y. Onodera, K. Nishino, A. Yamaguchi, Structural basis for the inhibition of bacterial multidrug exporters, Nature 500 (2013) 102–106, https://doi.org/10.1038/nature12300.
[23] M. Parmar, S. Rawson, C.A. Scarff, A. Goldman, T.R. Dafforn, S.P. Muench, V.L.G. Postis, Using a SMALP platform to determine a sub-nm single particle cryo-EM membrane protein structure, Biochim. Biophys. Acta 1860 (2018) 378–383, https://doi.org/10.1016/j.bbamem.2017.10.005.
[24] H. Akama, M. Kanemaki, M. Yoshimura, T. Tsukihara, T. Kashiwagi, H. Yoneyama, S. Narita, A. Nakagawa, T. Nakae, Crystal structure of the drug discharge outer membrane protein, OprM, of Pseudomonas aeruginosa: dual modes of membrane anchoring and occluded cavity end, J. Biol. Chem. 279 (2004) 52816–52819, https://doi.org/10.1074/jbc.C400445200.
[25] O. Lambert, H. Benabdelhak, M. Chami, L. Jouan, E. Nouaille, A. Ducruix, A. Brisson, Trimeric structure of OprN and OprM efflux proteins from Pseudomonas aeruginosa, by 2D electron crystallography, J. Struct. Biol. 150 (2005) 50–57, https://doi.org/10.1016/j.jsb.2005.01.001.
[26] F. Hagn, M. Etzkorn, T. Raschle, G. Wagner, Optimized phospholipid bilayer nanodiscs facilitate high-resolution structure determination of membrane proteins, J. Am. Chem. Soc. 135 (2013) 1919–1925, https://doi.org/10.1021/ja310901f.
[27] I.G. Denisov, S.G. Sligar, Nanodiscs in membrane biochemistry and biophysics, Chem. Rev. 117 (2017) 4669–4713, https://doi.org/10.1021/acs.chemrev.6b00690.
[28] Y. Li, A.Z. Kijac, S.G. Sligar, C.M. Rienstra, Structural analysis of nanoscale self-assembled discoidal lipid bilayers by solid-state NMR spectroscopy, Biophys. J. 91 (2006) 3819–3828, https://doi.org/10.1529/biophysj.106.087072.
[29] S. Bibow, Y. Polyhach, C. Eichmann, C.N. Chi, J. Kowal, S. Albiez, R.A. McLeod, H. Stahlberg, G. Jeschke, P. Güntert, R. Riek, Solution structure of discoidal high-density lipoprotein particles with a shortened apolipoprotein A-I, Nat. Struct. Mol. Biol. 24 (2017) 187–193, https://doi.org/10.1038/nsmb.3345.
[30] L. Daury, J.-C. Taveau, D. Salvador, M. Glavier, O. Lambert, Reconstitution of membrane proteins into nanodiscs for single-particle electron microscopy, Methods Mol. Biol. Clifton NJ 1635 (2017) 317–327, https://doi.org/10.1007/978-1-4939-7151-0_17.
[31] M.L. Carlson, J.W. Young, Z. Zhao, L. Fabre, D. Jun, J. Li, J. Li, H.S. Dhupar, I. Wason, A.T. Mills, J.T. Beatty, J.S. Klassen, I. Rouiller, F. Duong, The Peptidisc, a simple method for stabilizing membrane proteins in detergent-free solution, elife 7 (2018), https://doi.org/10.7554/eLife.34085.